






OPTICAL OBSERVATIONS OF SHOCK FILAMENTS IN TYCHO'S SUPERNOVA REMNANT

SLADJANA KNEŽEVIĆ¹ , STEVE SCHULZE² , JAIRO MÉNDEZ-ABREU^{3,4} ,
GLENN VAN DE VEN⁵  and GIOVANNI MORLINO⁶ 

¹*Astronomical Observatory, Volgina 7, 11060 Belgrade, Serbia*
E-mail: sknezevic@aob.rs

²*Center for Interdisciplinary Exploration and Research in Astrophysics (CIERA),
Northwestern University, 1800 Sherman Ave., Evanston, IL 60201, USA*

³*Instituto de Astrofísica de Canarias, 38205 La Laguna, Tenerife, Spain*

⁴*Departamento de Astrofísica, Universidad de la Laguna, 38206 La Laguna, Tenerife, Spain*

⁵*Department of Astrophysics, University of Vienna,
Türkenschanzstrasse 17, 1180 Vienna, Austria*

⁶*INAF/Osservatorio Astrofisico di Arcetri, Largo E. Fermi, 5 - 50125 Firenze, Italy*

Abstract. We present observations of the supernova remnant Tycho obtained with OSIRIS at the Gran Telescopio Canaria. With its large field-of-view ($4' \times 4'$), spatial sampling of $0.25''$ and spectral resolution of 650 km s^{-1} , we covered a large portion of the remnant and resolved the broad $\text{H}\alpha$ component ($\sim 1000 \text{ km s}^{-1}$). Previously, we observed the narrow ($\sim 10 \text{ km s}^{-1}$) and intermediate ($\sim 100 \text{ km s}^{-1}$) component in the same region using $\text{GH}\alpha\text{FaS}$ on the William Herschel Telescope. Observing all three line components at exactly the same locations along the filaments and applying shock models give more precise information on the overall conditions in the shock, and enable us to quantify cosmic-ray properties.

1. INTRODUCTION

In past decades, there has been a notable increase in research focused on observing and modeling optical emission originating in the supernova remnant (SNR) forward shock passing through partially ionized medium. This radiation is characterized by multiple-component Balmer-line profiles: narrow – emerging from upstream hydrogen cold atoms, intermediate – originating from hydrogen atoms heated in the neutral-induced precursor (downstream fast neutrals that overtake the shock), and broad – created in charge exchange reactions between downstream hot protons and the upstream cold atoms. By analyzing these profiles, we can gain a deeper understanding of the ambient medium conditions, the shock structure and the acceleration of cosmic rays (CRs), providing valuable insights into the evolution and energetics of SNRs (Morlino et al. 2012, 2013).

Current shock models (Blasi et al. 2012; Morlino et al. 2012, 2013) include neutral-induced and CR precursor effects on the shock structure and line profiles. In addition, increased efforts in the past decade were directed towards untangling physical and geometrical effects to ensure an accurate interpretation of the data (Raymond et al. 2007; Bandiera et al. 2019). Alongside theoretical advancements, observations have

also intensified, leading to the acquisition of high-resolution images and spectra (e.g., Nikolić *et al.* 2013; Knežević *et al.* 2017, 2021).

In this paper we report the results of Tycho’s SNR observations with the **O**ptical **S**ystem for **I**maging and low-**I**ntermediate-**R**esolution **I**ntegrated **S**pectroscopy (**OSIRIS**), an imager and spectrograph for the optical wavelength range, on the 10.4 m Gran Telescopio Canarias (GTC).

2. OBSERVATIONS AND DATA REDUCTION

We used the GTC/OSIRIS instrument in the narrow-band tunable filter (TF) imaging mode, which is in essence a low resolution Fabry-Pérot etalon. OSIRIS uses two CCDs (2048×4102 pixel each) to cover its total field-of-view (FoV) of $8' \times 8'$ with an image scale of $0.125''/\text{pixel}$. However, the standard observing mode uses $0.254''$ binned pixels and a FoV of $4' \times 4'$. Our observations of the northeastern (NE) rim of Tycho’s SNR (left panel in Figure 1) were performed on 20 November 2011, 21-22 January and 15 September 2012. All observations were conducted under seeing $\leq 1.20''$, photometric or clear conditions, dark moon, and airmass ≤ 1.88 . The pointing was centered at $\alpha_{J2000} = 0^h 26^m 4^s.5$, $\delta_{J2000} = 64^\circ 09' 44''$. The central wavelength of the TF was chosen to be in the range 650–670 nm (with a width of 1.3–1.7 nm), which places the targeted H α line in the middle of this interval. We did 34 narrow-band scans (each 5 min), so that, including the overheads, the total exposure time was 7 hours.

Data reduction was accomplished for each CCD separately. Bias correction was done by creating a median of all Bias frames in one observational block (OB), and was subtracted from every exposure separately. TF Flat Fields were obtained using Dome Flats, with the TF tuned to the same wavelengths as the science observations (5 Dome Flats exposures of 1-3s at each wavelength). The flatfield model was then created as a median of all Dome Flats within one OB. Due to the OSIRIS etalon being positioned in a converging beam, the effective wavelength varies across the FoV increasing radially from the optical center. This increase produces rings of constant wavelength with respect to the TF center located nearly in the middle of the detector system. As a result, pixels with different positions will have different effective wavelengths, unless they are at the same distance from the optical center. Thus, for every given wavelength at the optical center and every pixel position we had to calculate the effective wavelength (see Méndez-Abreu *et al.* 2011). The instrument profile is Lorentzian with a width of around 650 km s^{-1} . Data were flux calibrated with respect to the observed standard star G191-B2B. Prior to median combining images of the same wavelength, they underwent astrometric calibration.

To account for sky/background (bkg later in the text) emission every exposure was fitted with a 2D polynomial of order of 12 in x-direction and 20 in y-direction. The bkg model was constructed as a median of all the individual bkg-exposure models with the same central wavelength.

3. DATA ANALYSIS AND RESULTS

The same portion of the Tycho’s SNR was observed with the GH α FaS instrument on the William Herschel Telescope in La Palma (Knežević *et al.* 2017), where we resolved the narrow-line’s (NL) full-width at half-maximum (FWHM) of $\sim 10 \text{ km s}^{-1}$. The observations revealed suprathermal NL widths ($\gg 20 \text{ km s}^{-1}$) and an intermediate-

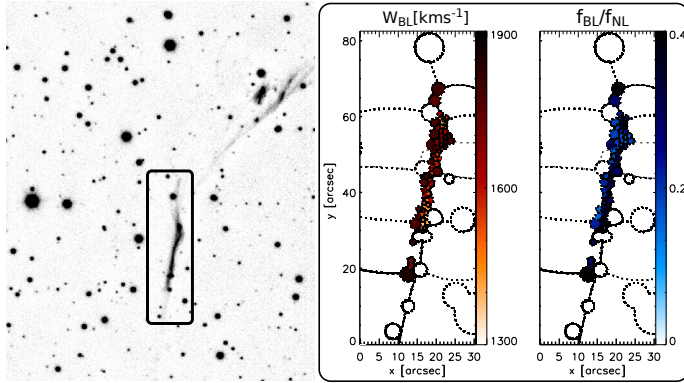


Figure 1: Left panel: reduced and bkg subtracted OSIRIS image at the $H\alpha$ central wavelength. Middle and right panel: zoom-in onto the eastern filament showing spatial variation of the BL width (W_{BL}) and broad-to-narrow flux ratio (f_{BL}/f_{NL}).

line (IL) component with 180 km s^{-1} average width. With the OSIRIS instrument we resolve the broad-line (BL) component with $\text{FWHM} \sim 1000 \text{ km s}^{-1}$.

Here we present the same Bayesian analysis as described in Knežević et al. (2017), but on the OSIRIS data independently from the GHαFaS data. The locations of the bins from which the spectra were extracted correspond to exactly the same locations in both datasets. We define a model as a sum of a shock emission described with 2 Gaussian components (one for NL and one for BL) and a bkg model. To constrain the NL's width W_{NL} , we employed a prior distribution with a range of $[15, 100] \text{ km s}^{-1}$. This range encompasses the pre-shock temperature of approximately 5000 K and the maximum predicted W_{NL} based on the Morlino et al. (2013) shock model, which accounts for the emission from the CR precursor. W_{BL} was defined in the range $[1000, 3500] \text{ km s}^{-1}$. We did not express a strong preference for any particular parameter values within the model definition limits. This was achieved by employing Dirichlet and Beta prior distributions with a shape parameter of 1.5 for the model parameters (flux fractions in the lines, log-line widths, NL centroid, and BL offset from the NL centroid). The likelihood follows Gaussian distribution. To draw samples from the posterior we use Markov chain Monte Carlo (MCMC) following Knežević et al. (2017).

Figure 2 shows parameter estimation for one of the bins. All parameters seem well constrained apart from the NL width that is unresolved with the OSIRIS spectral resolution of 650 km s^{-1} . In the shown example estimated BL parameters are $f_{BL} \approx 0.22$, $\Delta\mu_{BL} \approx 600 \text{ km s}^{-1}$ (centroid separation between BL and NL), and $W_{BL} \approx 1342 \text{ km s}^{-1}$. Middle and right panels in Figure 1 show spatial variation of W_{BL} and broad-to-narrow flux ratio f_{BL}/f_{NL} in the eastern filament, where $W_{BL} \approx 1630 \text{ km s}^{-1}$ and $f_{BL}/f_{NL} \approx 0.27$ on average. Smaller widths than previously measured in the brightest knot in this filament ($1800\text{--}2400 \text{ km s}^{-1}$; e.g. Smith et al. 1994; Raymond et al. 2010) might indicate efficient CR acceleration, something we already found evidence for in GHαFaS data where we measured suprathermal NL widths. In fact, smaller BL widths correspond to a smaller plasma temperature, suggesting that a fraction of the shock kinetic energy is channeled into accelerated particles rather than into the thermal component. However, before making any conclusions, we should first do the analysis for the model containing IL and/or two BLs since the reason for measuring smaller

widths might be connected to the complex shock geometry. Also, we note that we might be overestimating bkg emission and the result should be checked if different bkg models influence the outcome.

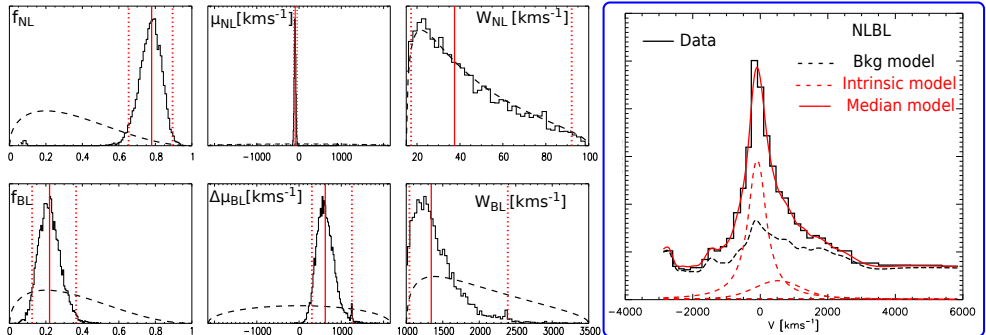


Figure 2: Parameter estimation for the bin in the eastern filament of Tycho’s SNR. Smaller panels show marginalized posteriors of individual model parameters (solid lines): flux fractions in the lines (f_{NL} , f_{BL}), NL centroid (μ_{NL}), BL offset from the NL centroid ($\Delta\mu_{\text{BL}}$), and intrinsic line widths (W_{NL} , W_{BL}). Overplotted dashed lines are prior distributions. W_{NL} is unconstrained due to the instrument’s insufficient spectral resolution. Solid-red vertical lines are medians of the posterior distributions, and dotted-red vertical lines are the 95% confidence intervals. The large blue panel shows the data as a histogram, the background model as a dashed-black line, shock emission components as dashed-red, and the median model as a solid-red line.

4. SUMMARY AND FUTURE WORK

We presented GTC/OSIRIS observations of the NE region in Tycho’s SNR where we have resolved broad $\text{H}\alpha$ component. Bayesian inference was applied in order to obtain reliable parameter estimates. We measured BL width of 1630 km s^{-1} and broad-to-narrow flux ratio of 0.27 on average in the entire NE rim. In addition to incorporating more sophisticated models, the analysis should be performed simultaneously on $\text{GH}\alpha\text{FaS}$ and OSIRIS datasets. This will enable us to deduce the shock’s geometry and investigate physical phenomena using shock models.

Acknowledgments

S. K. acknowledges the financial support of the Ministry of Science, Technological Development and Innovation of the Republic of Serbia through the contract No. 451-03-66/2024-03/200002.

References

- Bandiera, R., Morlino, G., Knežević, S., et al.: 2019, *MNRAS*, **483**, 1537.
 Blasi, P., Morlino, G., Bandiera, R., et al.: 2012, *ApJ*, **755**, 121.
 Knežević, S., Läsker, R., van de Ven, G., et al.: 2017, *ApJ*, **846**, 167.
 Knežević, S., Morlino, G., Bandiera, R., et al.: 2021, *Publ. Astron. Obs. Bel.*, **100**, 267.
 Méndez-Abreu, J., Sánchez Almeida, J., Muñoz-Tuñón, C., et al.: 2011, *PASP*, **123**, 1107.
 Morlino, G., Bandiera, R., Blasi, P., et al.: 2012, *ApJ*, **760**, 137.
 Morlino, G., Blasi, P., Bandiera, R., et al.: 2013, *ApJ*, **768**, 148.
 Nikolić, S., van de Ven, G., Heng, K., et al.: 2013, *Science*, **340**, 45.
 Raymond J. C., Korreck K. E., Sedlacek, Q. C., et al.: 2007, *ApJ*, **659**, 1257.
 Raymond, J. C., Winkler, P. F., Blair, W. P., et al.: 2010, *ApJ*, **712**, 901
 Smith, R. C., Raymond, J. C., Laming, J. M.: 1994, *ApJ*, **420**, 286.